Dynamic Light Scattering and Small-Angle Neutron Scattering Studies of Ternary Rod/Coil/Solvent Systems

Edward T. Hanson

Department of Chemistry, Stanford University, Stanford, California 94305-5080

R. Borsali

LCPO-CNRS-ENSCPB-Bordeaux University (UMR5629), Avenue Pey-Berland, BP 108-33402 Talence Cedex, France

R. Pecora*

Department of Chemistry, Stanford University, Stanford, California 94305-5080

Received October 30, 2000; Revised Manuscript Received January 8, 2001

ABSTRACT: Dynamic light scattering (DLS) and small-angle neutron scattering (SANS) are used to characterize the structure and dynamics of ternary solutions consisting either of rods or "hairy rod" polymers and polystyrene (PS) coils in a solvent composed of chloroform saturated with (<0.5%) formamide (CF). The rods are poly(γ-benzyl-α-L-glutamate) (PBLG), and the hairy rods are two forms of poly(γ-octadecyl-α-L-glutamate)-*co*-(γ-methyl-α-L-glutamate) with varying amounts of octadecyl substitution. The DLS autocorrelation functions reveal the existence of two relaxation modes that are interpreted in terms of the random phase approximation theory (RPA) as the cooperative and interdiffusive modes. The two relaxation modes are investigated as a function of the total polymer concentration C_P and the relative composition $x = C_{rod}/C_P$ as well as the percentage of octadecyl groups along the polyglutamate chain. The different diffusion coefficients that characterize the dynamics in these systems are well described by the RPA theory of polymer mixtures. In addition, the interaction parameter χ extracted from both the DLS and SANS experiments is found to be negative. These results suggest an attraction between PS and PBLG molecules and that these polymers are therefore compatible. The hairy rod ternary solution diffusion coefficients indicate that as the percentage of hairs on the rod increases, the polymers become more compatible.

I. Introduction

The study of polymer mixtures is a burgeoning area of polymer science, and much work is currently directed at understanding the molecular structure and interactions in these mixtures. Scattering techniques, in particular, are important tools in the investigation of the structure and dynamics of ternary polymer (1)/polymer (2)/solvent solutions. The random phase approximation (RPA), which has recently been reviewed by Borsali,[1] has been successful in interpreting scattering experiments on these systems and obtaining important solution parameters from the data. Earlier work in the study of ternary polymer solutions usually required that the system studied be specially designed in order to make interpretation of the experimental results tractable. For static and dynamic light scattering experiments from ternary systems, this has usually meant choosing a solvent that is isorefractive with one of the two polymer components. The second polymer is then used as a probe in the invisible matrix, and the interpretation of the results is thus much easier. Many different types of ternary systems have been studied using refractive index matching, including the especially interesting case in which one of the polymer components is a rodlike polymer.[2,3] In these rod/coil/solvent studies,[2,3] polystyrene was used as the "visible" probe in an isorefractive solution of rods.

There are two diffusive modes expected from the RPA for ternary polymer solutions. These two modes are often identified as the cooperative and interdiffusion modes (see ref 1 and references therein). The frequencies and amplitudes of these modes are given by the RPA in terms of polymer and solvent properties. For probe diffusion studies, small amounts of probe usually lead to a single diffusion process that can be identified as the probe self-diffusion. As the ratio of visible polymer to index matched polymer increases, the second mode increases in amplitude and becomes observable. A number of experiments have been done to study the dynamics of coil (1)/coil (2)/solvent under various experimental conditions and compare the results with the predictions of the RPA. For compatible polymers, a wide range of molecular weights and concentrations has been investigated. The self-diffusion coefficients and the polymer−polymer interaction parameter are the most useful quantities that can be determined using the RPA model.

The RPA has been also developed for rodlike polymers by Doi, Shimada, and Okano (DSO) in a series of papers.[4,5] The main addition to the normal RPA is the inclusion of a nematic potential which accounts for parallel rod−rod interactions. Isotropic solutions of rodlike polymers become unstable at high enough concentrations because of these nematic interactions. The DSO theory specifically treats semidilute binary solutions of rodlike polymers, and rod/coil/solvent systems have previously been studied only under refractive index matching conditions.[2,3] Most of the experiments done with respect to ternary polymer systems deal with coil (1)/coil (2)/solvent systems.

We study here the structure and dynamics of two different types of rod/coil/solvent systems and analyze

10.1021/ma001857j CCC: $20.00
Published on Web 02/23/2001

the results in terms of the RPA. Our objectives are to test the consistency of the RPA for these rod/coil/solvent mixtures and to then use it to extract interaction parameters for the particular systems studied. The first system is a series of ternary polymer solutions of rod/coil/solvent in which the total polymer concentration is kept constant, and the relative amounts of rod and coil are varied from 0% to 100%. The rigid rod is the α-helical polypeptide poly(γ-benzyl-α-L-glutamate) (PBLG). It is one of the most rigid synthetic polymers known. This system is studied using both DLS and SANS. The second system is a series of ternary solutions of "hairy" rod/coil/solvent, in which the total polymer concentration is varied while the hairy rod concentration is kept at 5% of the total polymer concentration. Hairy rodlike polymers [poly(γ-methyl-α-L-glutamate)-*co*-(γ-octadecyl-α-L-glutamate)] were used in which the fraction of monomers with octadecyl groups ("hairs") was 30% and 60% for the two different polymers. In all experiments, the flexible coil polymer is polystyrene (PS), and the solvent is chloroform saturated with (<0.5%) formamide (CF). Formamide is added to the chloroform to prevent aggregation of the rods.[6] In CF solvent both components are "visible", so that theories which take this into account are necessary to interpret the results.

II. Experimental Section

The polystyrene was purchased from Polymer Standards Service-USA (lot PS19121). It was DIN certified; i.e., it was characterized by gel permeation chromatography (GPC), static light scattering, and viscometry, and values of the characterization parameters were provided to us by PSS-USA. The reported $M_w = 9.51 \times 10^5$g/mol (static light scattering) and $M_w/M_n = 1.07$ (GPC). The poly(γ-octadecyl-α-L-glutamate)-*co*-(γ-methyl-α-L-glutamate) (hairy rods) were synthesized by Hilde von Esbroeck and Curtis Frank of the Stanford University Chemical Engineering Department and were studied in binary solutions previously.[7] Two hairy rod polymers are used here. They are called HB and HC below and have stearyl percentages of 60%, and 30%, respectively. Their contour lengths are respectively estimated to be 68 and 78 nm. The poly(γ-benzyl-α-L-glutamate) (PBLG) was purchased from Sigma Chemical Company (lot 91H5521) with a reported $M_w = 1 \times 10^5$ g/mol by low-angle light scattering and reported $M_v = 1.18 \times 10^5$ g/mol from viscosity measurements.

Ternary hairy rod/coil/solvent and binary polystyrene/solvent samples were prepared by serial dilution for DLS experiments. For the PBLG/PS/CF DLS experiments, appropriate amounts of stock solutions (each 16 mg/mL) were added to make solutions of each composition, allowing several days for equilibration. Each solution was centrifuged at 12 000 rpm for at least 3 h and transferred to dust-free cuvettes for DLS experiments.

The DLS autocorrelation functions were measured at scattering angles of 60°, 90°, and 120° for most samples using an apparatus described previously,[8] except that a BI9000 (Brookhaven) multiple sample time correlator was used. A few samples were measured at more scattering angles to observe more closely the q dependence of the relaxation modes. Inverse Laplace transforms of the data were performed using Provencher's FORTRAN program CONTIN,[9] and diffusion coefficients were determined from the slope of the relaxation frequencies (Γ) vs q^2.

The SANS experiments were performed at the National Institute of Standards and Technology Cold Neutron Research Facility (NIST-CNRF) on the 30 m neutron scattering instrument (NG-3). The range of the scattering vector length q was from 0.003 to 0.15 Å^{-1}. This wide range was obtained using two experimental configurations. In the low-q configuration, the neutron wavelength (λ) was 5 Å and the detector was set at 10.55 m from the sample. For the higher q range, $\lambda = 6$ Å and the detector was set at 3.55 m. Deuterated chloroform was used to provide good contrast between the polymer and solvent. The data reduction was performed according to NIST standard procedures, including empty cell and blocked beam subtractions and transmission corrections. The attenuated direct beam was used to put the data on an absolute scale. The samples used for small-angle neutron scattering (SANS) were prepared in a similar way to the light scattering samples, except the total polymer concentration was 32.2 mg/mL and deuterated (99.8% D) chloroform from ICN Biomedicals (lot 87557) was used.

Most of the measurements described here were done at 25 °C. In cases where they were done at other temperatures, those temperatures are indicated at the appropriate point in the text.

III. DLS Binary Solution Results

A. Polystyrene. The binary system of polystyrene in chloroform saturated with formamide was studied first. The polymer has a reported $R_g = 48.9$ nm in THF at 25 °C, which gives an estimate of the overlap concentration, $C^* = 3.2$ mg/mL. An estimate of C^* can also be made from the intrinsic viscosity [η]. The intrinsic viscosity reported by Polymer Standards Service is 225.5 mL/g for the polystyrene in THF at 30 °C. We measured the intrinsic viscosity of the polystyrene in chloroform saturated with formamide at 25 °C and obtained 253.9 ± 7.4 mL/g. This gives an overlap concentration of $C^* \cong 1/[\eta] = 3.9$ mg/mL. The range of concentrations studied covers the crossover from dilute to semidilute solutions. The series of concentrations investigated range from 0.8 to 20 mg/mL, which corresponds to $0.25C^*$ to $6.2C^*$, assuming that the R_g value in chloroform/formamide at 25 °C is the same as the reported R_g (in THF). These values are expected to be similar since chloroform is a good solvent for polystyrene.[10]

There is one major relaxation mode in the DLS autocorrelation functions from binary solutions of PS/solvent. CONTIN analysis shows that this process always contributes over 90% of the amplitude of the relaxation. (The weaker relaxation is discussed in detail below.) The frequency Γ of the major relaxation is found to be q^2-dependent in all investigated concentrations. The highest 20 mg/mL and lowest 0.8 mg/mL concentration solutions were measured at several scattering angles to detect any deviation from q^2 dependence. Figure 1a shows no deviation from the linear fit for Γ vs q^2 for the 20 mg/mL solution. The slope gives the cooperative diffusion coefficient. For each concentration, the diffusion coefficient was determined from the slope of similar Γ vs q^2 plots. Figure 1b shows the cooperative diffusion coefficients for the binary solutions of polystyrene over the range of concentrations studied. A log−log plot of the data at C^* and above has a slope of 0.52, which is in agreement with data for polystyrene in other good solvents[11,12] and should be compared to the theoretical value from scaling laws of 0.75.[13] Theoretically, an exponent of 0.5 is expected for a marginal solvent. It has been suggested that the 0.75 exponent may be reached for higher molecular weight polymers. It is also worth noting that the C^* can be estimated from the log−log representation of D vs C at the crossover (see Figure 1b). For our system, this gives $C^* = 3.5$ mg/mL, in good agreement with the calculated value and the one deduced from the viscosity measurements.

Many studies of flexible coil polymers in dilute to semidilute solutions have identified a bimodal (or multimodal) relaxation of the autocorrelation function. In this study, we observe a second relaxation in many of

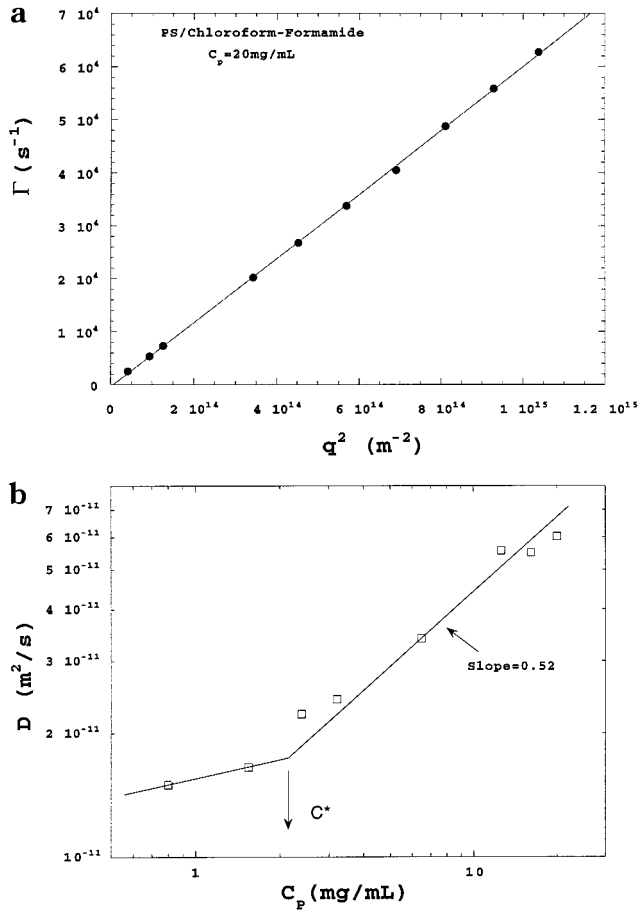

Figure 1. (a) The main relaxation frequency for the polystyrene solution at 20 mg/mL in chloroform/formamide. The slope of the line gives the translational diffusion coefficient. (b) The mutual diffusion coefficient of polystyrene as a function of the concentration. The semidilute solution scaling law is indicated as the solid line.

the solutions. In the dilute regime, for $qR_g < 1$, the single relaxation mode gives the translational diffusion coefficient. For dilute solutions above $qR_g = 1$, the translational diffusion mode is still the main mode, with over 90% of the amplitude. Dilute solutions of flexible polymers can be described as a collection of independent coils, with a diffusion coefficient, D_T, characterizing the translational diffusion. Above $qR_g = 1$, the length scale investigated by DLS ($1/q$) becomes comparable to the length scale of the polymer (R_g), and internal modes of motion of the polymer become accessible to the DLS measurements. At roughly $qR_g = 1$, one internal mode has a measurable, but relatively small, amplitude. The internal modes are faster than the translational diffusion mode and are easily separated in this case by the inverse Laplace transform program, CONTIN.[9] Stockmayer and Hammouda have reviewed the dynamics of dilute solutions of flexible polymers, including the $qR_g > 1$ regime.[14]

Semidilute solutions of flexible coils form a transient network of overlapping polymer chains. In the semidilute regime, for $qR_g < 1$, the single relaxation mode gives the cooperative diffusion coefficient. For $qR_g > 1$, the major mode of relaxation is still cooperative diffusion, with over 90% of the amplitude, but there is also a slow mode. The slow mode is not observed in all autocorrelation functions. It appears most often and with the greatest amplitude in the samples that are the most concentrated and at the highest scattering angles. The slow mode is discussed further below. The diffusion coefficient obtained from the fast mode is, as stated above, identified with the cooperative diffusion coefficient D_c. The dynamic correlation length (ξ_e) can be used to characterize the polymer network in terms of the hydrodynamic screening and is calculated from D_c by

$$\xi_e = kT/6\pi\eta D_c \qquad (1)$$

Brown and Nicolai[15] review the static and dynamic properties of semidilute solutions of flexible polymers in good (and Θ) solvents. In this review, they construct a universal curve for ξ_e for polystyrene in various good solvents in the semidilute concentration regime, including a wide range of molecular weights. The equation for this curve is given by $\xi_e = (0.53 \pm 0.1)C^{-0.70\pm0.01}$ nm, with C the concentration in g/mL. Our data fall within the given range for 20 mg/mL ($C/C^* = 6.2$) but are 5% and 10% below the minimum in the given range for $C/C^* = 3.9$ and 2, respectively.

B. Polystyrene Slow Mode. In this section, we discuss the polystyrene/CF slow mode in some detail in order to distinguish it from the slow mode observed in the ternary solutions.

There has been a significant amount of work done on semidilute solutions of flexible polymers, and polystyrene is one of the most studied. There has been much discussion concerning the characterization and identification of the slow modes. There are two main types of slow modes found in semidilute polymer solutions. These are distinguished by the dependencies of their relaxation frequencies on the scattering vector q. Many slow modes have been shown to have relaxation frequencies proportional to the square of the scattering vector. This q^2 dependence indicates that the mode is diffusive. Another type of slow mode has been shown to have a relaxation frequency that is independent of the scattering vector and is referred to as a viscoelastic mode. For either class of slow mode, the mode amplitude increases as the concentration is increased.

Some authors have identified a q^2-dependent slow mode as the self (or polymer center-of-mass) diffusion coefficient.[16−18] Part of this identification is based upon the concentration dependence of the slow mode frequency being consistent with the scaling law predictions of de Gennes for the self-diffusion coefficient:[11] $D_{self} \sim C^{-1.75}$. This scaling behavior for the self-diffusion coefficient assumes reptation of the flexible polymer. Independent measurements of self-diffusion coefficients by pulsed field gradient NMR[19,20] (PFG-NMR) and by forced Rayleigh scattering[21,22] show, however, that the self-diffusion coefficient is 1−2 orders of magnitude slower than the diffusion coefficient calculated from the slow mode. Brown et al. did both PFG-NMR and DLS measurements on the same samples and showed that D_{self} from PFG-NMR is about 1 order of magnitude faster than the DLS slow mode.[23,24] Many of these experiments did verify the scaling law, but some over only a limited range of concentrations.

Many researchers have identified the q^2-dependent slow mode as the translational diffusion coefficient of clusters of segments. Supporting this interpretation is the fact that slow modes are more commonly found in, and tend to have larger amplitudes in, Θ solvents. Brown and Stepánek used a very large range of temperatures (−44 to 70 °C) to explore the transition from Θ to moderately good solvent.[25] Although it should be

noted that they observed two slow modes, the total amplitude of the slow modes greatly decreased as the solvent quality increased. As the solvent quality is decreased, it is expected that polymer solutions should tend toward the formation of clusters. Further evidence for cluster formation comes from a combination of dynamic and static light scattering experiments.[26,27] The mean-square radius of gyration measured by static light scattering increases rapidly above C^* as the slow mode becomes apparent in DLS. A proposed explanation of the slow mode[22] is that there is a transient network of loosely entangled polymer chains whose motion is highly restricted. The entire cluster cannot diffuse together, but by dissociation of individual chains, likely by reptation, and by reassociation into another cluster, the original cluster would appear to move.

A q-independent mode has been identified by many authors as a viscoelastic mode. Recently, Delsanti et al. have given a good description of the viscoelastic mode.[28] In semidilute polymer solutions, the polymers form temporary networks that give the solution elasticity, within a solvent that takes up the rest of the volume. Two types of forces affect the polymer motion: a viscous force, from polymer−solvent interactions, and a restoring force, which includes both an osmotic and an elastic term. The elastic force is related to the longitudinal stress modulus $M(t)$ of the polymer network. The solution is often referred to as a pseudogel. The system behaves like a gel at short times, since the polymer network remains essentially the same over the time of interest. But at long times the solution behaves like a liquid, since the network has enough time to rearrange many times.

Wang has developed a treatment of the viscoelastic mode, whose main parameter, β, gives the coupling of the polymer concentration fluctuation to the solution viscoelasticity.[29,30] This coupling parameter is proportional to the change in density of the solution as polymer is added. To demonstrate this dependence, Wang et al. studied semidilute, isopycnic solutions of polystyrene in diethyl malonate (Θ solvent) and found no slow mode.[31] Brown and Stepánek chose four different Θ solvents for polystyrene with different β values.[32] When the data are scaled with temperature and viscosity, the four autocorrelation functions are superimposable, including the observed slow mode. Also, a binary solvent (75% diethyl phthalate/25% dioctyl phthalate) was used to reach $\beta = 0$, with the slow, viscoelastic mode still appearing. These authors also point out that the theory of Wang does not include predictions for the concentration or molecular weight dependence of either the amplitude or the frequencies of the viscoelastic mode, despite the experimental evidence of their relationship.[13] The viscoelastic modes have been found to be much more important and dominant for Θ solvents. In poor solvent systems, there are several viscoelastic modes that span a very large frequency range.

In light scattering experiments different distance and time scales are probed by choosing a range of scattering vector lengths (q). Adam and Delsanti performed experiments over a wide range of q in good solvents for dilute to semidilute solutions.[33] The regimes are divided according to the reduced quantities qR_g and C/C^*. The semidilute regime, $C/C^* > 1$, is divided into three regimes depending on the scattering vector length. If $qR_g < (C/C^*)^{-1.125}$, the solution can be treated as a liquid and the autocorrelation function should decay according to a single q^2-dependent mode that gives the mutual diffusion coefficient, D_m. In the intermediate range $(C/C^*)^{-1.125} < qR_g < (C/C^*)^{0.75}$, semidilute polymer solutions behave like polymer networks swollen by solvent. The single decay mode should be q^2 dependent and give a cooperative diffusion coefficient, D_c. The dynamic correlation length can be calculated from D_c and eq 1 and is identified as being the mesh size of the network. At high scattering vectors $qR_g \gg (C/C^*)^{0.75}$, the internal structure of the network is investigated; this boundary is alternatively indicated by $q\xi > 1$. There should be one relaxation frequency (Γ) given by[31]

$$\Gamma = \frac{kT}{6\pi\eta} q^3 \tag{2}$$

where k is Boltzmann's constant, T the kelvin temperature, and η the solvent viscosity. It should be noted that Γ is independent of the polymer molecular weight and concentration in this regime. When hydrodynamic interactions are considered, the constant 6 becomes $6\sqrt{2}$.[31] Using high molecular weight polystyrene at $qR_g \geq 4.4$, Adam and Delsanti observed a single relaxation whose decay rate is close to that given by eq 2. From a log−log plot, they found the q exponent to be 2.85 ± 0.05. Using this scaling exponent, they determined 0.51 ± 0.03 for the exponent α in the D_c vs C^a relation,[31] which is the same as our observed value.

The experiments of Adam and Delsanti covered many regimes in the dynamics of flexible polymers in good solvents. The data were all fit to single exponentials, and therefore the discovery and identification of low-amplitude additional modes would not be expected. The systems were chosen as examples of the various regimes of interest. It was only theoretically, and with reference to de Gennes-like scaling laws, that the crossover between regimes was discussed. In similar experiments exploring the dynamics of flexible polymers in Θ solvents, multimodal analysis has been required, and it has been noted that the transitions between the regimes are not sharp.[34,35]

The slow mode observed in the current study is not clearly defined with respect to previously observed slow modes. In Figure 2a, we show the variation of the amplitudes of the slow mode as a function of q^2. Note that at scattering angles below 60° no slow mode is observable. The frequency Γ_s/q^2 associated with the slow mode is plotted in Figure 2b as a function of q. The slope of the linear fit, 3.636×10^{-19} m^3/s, can be compared to the coefficient in eq 2. From the experimental conditions $T = 298.15$ K and $\eta = 0.5357$ cP, the coefficient in eq 2 is 4.077×10^{-19} m^3/s (and 2.884×10^{-19} m^3/s with the hydrodynamic interaction correction). Equation 2 is the result of considering only very large scattering vectors with respect to the coil radius. The break from a single mode to two modes occurs very close to $qR_g = 1$. There are very large errors associated with the amplitude and decay rate of the slow mode because of its small amplitude. At the concentration of 20 mg/mL ($6.2C^*$), the crossover to the liquidlike regime should be at $qR_g = (C/C^*)^{-1.125} = 0.13$, which is significantly below all experimental values of qR_g as can be seen in Table 1. Similarly, the regime in which only internal structure should be observed, $qR_g \geq (C/C^*)^{0.75} = 3.9$ or $q\xi \geq 1$, is also not even close to the experimental range probed. It is expected that all angles for PS at 20 mg/mL should be within the intermediate range where the polymer network is explored.

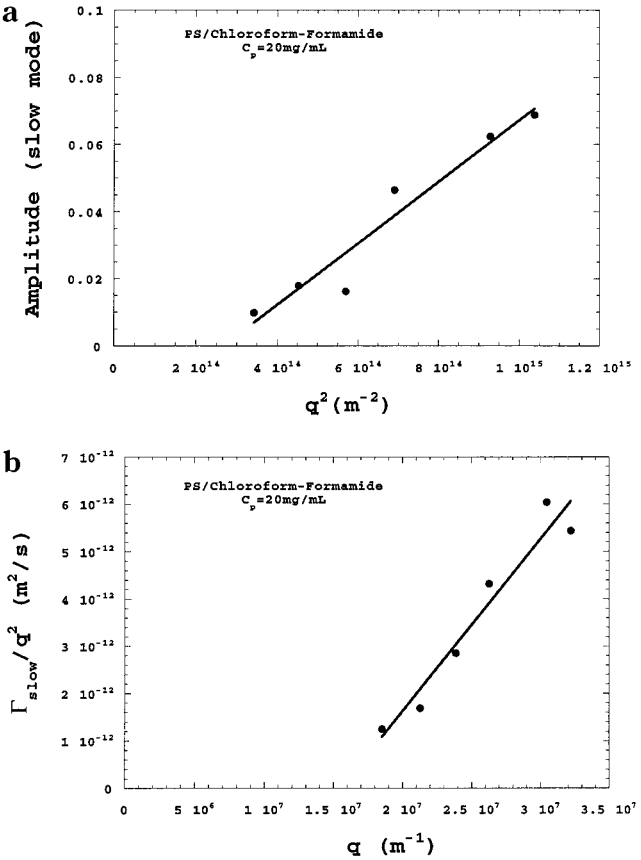

Figure 2. (a) The average relative amplitudes of the DLS slow mode for the 20 mg/mL polystyrene solution. Only the nonzero amplitudes were averaged. A linear fit is shown. (b) The DLS slow mode frequency for the 20 mg/mL polystyrene solution divided by the square of the scattering vector length. A linear fit is shown.

Table 1. Length Scales Associated with the Binary Polystyrene Solutions

angle (deg)	scattering vector length ($\times 10^7$ m)	qR_g	$q\xi$
20.1	0.649	0.318	0.0448
30.2	0.968	0.473	0.0668
35.3	1.13	0.550	0.0776
59.8	1.85	0.906	0.128
69.9	2.13	1.04	0.147
79.9	2.39	1.17	0.165
90.0	2.63	1.28	0.181
100.1	2.85	1.39	0.196
110.1	3.05	1.49	0.210
120.2	3.22	1.58	0.222

To further test the relationship in eq 2, the 20 mg/mL PS solution was measured at a scattering angle $\theta = 120°$ (maximum slow mode amplitude) over a range of temperatures from 10 to 40 °C (in 5 °C increments). Two relaxation modes were found at all temperatures, with the minor peak contributing 6.7−7.8% of the total amplitude. The major peak gave the same hydrodynamic radius (±0.5%) at all temperatures, as expected for a good solvent. The hydrodynamic radius of the minor peak was, within error, the same at all temperatures; the average error in the minor peak is 15%. The constant hydrodynamic radius of the slow peak as a function of the temperature indicates that Γ_{slow} is proportional to T/η, consistent with eq 2.

It is difficult to explain why there would be a q^3-dependent mode in the intermediate scattering vector regime. A very similar q^3 mode has been predicted[36−38] and observed[39,40] in dilute solutions, although in this case it is the fast mode. In dilute solutions, this type of mode is expected for $qR_g \gg 1$ and is identical to eq 2 except for a numerical factor (replace $1/6\pi$ with either 1/16,[34] 0.0788,[34] or 0.55[36]).

Although the origin of the slow mode in the binary polystyrene/chloroform (with formamide) semidilute solutions is not yet clear, there are some important characteristics of this mode, which make it quite distinct from the slow mode identified in the ternary polymer solutions. The amplitudes of the binary, semidilute slow mode increase strongly with scattering vector. The binary slow mode frequency is proportional to q^3, as opposed to the q^2 dependence for typical diffusive motion observed in the ternary solutions. The other important difference is that for the binary solutions the slow mode is found at high concentrations with a small amplitude. The experiments described below on the ternary systems show a second mode even at very low concentrations. So at least there are not likely to be contributions of the binary slow mode in the dilute ternary systems. As the concentration is increased, the binary slow mode is likely present but with a small amplitude and is probably hidden by the interdiffusion mode, which we note below exhibits a large amplitude.

C. Hairy Rods and PBLG. The structure and dynamics of these hairy rod polymers in binary solutions have been studied previously.[7] The translational diffusion coefficients were determined over a range of concentrations from the dilute to the semidilute using DLS. The diffusion coefficients show an initial decrease followed by an increase as the polymer concentration is increased. These results are discussed below and compared to those for the ternary solutions.

The DLS autocorrelation function of the scattered light intensity for the PBLG solution at 16.12 mg/mL fits a single exponential very well, and only one peak appears in the CONTIN analysis. As expected for a diffusive peak, the relaxation rate Γ is q^2-dependent. The mutual diffusion coefficient and the dynamic correlation length were determined from the slope of a Γ vs q^2 plot: $D_m = (4.75 \pm 0.01) \times 10^{-11}$ m^2/s and $\xi_e = 8.54$ nm. The dynamic correlation length can be compared to that for the similar size PBLG rod studied by Tracy and Pecora.[8] The current measurement gives a ξ_e that is about 5% less than would be expected from an interpolation of their ξ_e as a function of concentration. This comparison of ξ_e takes into account the viscosity of the different solvents, but it is still assumed that the solvent quality is the same for PBLG in both solvents. Tracy and Pecora[8] determined the translational diffusion coefficient of PBLG in dilute to semidilute DMF solutions using dynamic light scattering. The translational diffusion coefficient showed similar behavior to that of the hairy rods discussed, except that the initial decrease in the diffusion coefficient was much less drastic.

IV. DLS Ternary Solution Results

A. Random Phase Approximation. The RPA is used here to analyze the DLS experiments on the ternary polymer solutions. The theory has been developed over the past few decades by a number of researchers, including Edwards, De Gennes, Benoit, Akcasu, and Benmouna. Borsali[1] has recently given a detailed review of the development and the use of the RPA in the analysis of ternary polymer solutions.

For semidilute ternary polymer (1)/polymer (2)/solvent solutions, the dynamic structure factor $S_T(q,t)$ is expected to be a sum of two exponentials:

$$S_T(q,t) = A_1 \exp[-\Gamma_1 t] + A_2 \exp[-\Gamma_2 t] \quad (3)$$

where, as usual, q is the scattering vector and t the time. The amplitudes and decay rates of the normal modes are A_1, A_2 and Γ_1, Γ_2, respectively. In general, the amplitudes and decay rates of the normal modes depend on q. The complete equations for the two modes are given by Borsali[1] (eqs 43−45) under the assumption that the solvent quality is the same for both polymers and that the interaction between monomers can be taken into account by the χ parameter. The excluded-volume parameters are very different for the PBLG and PS used in this study, so the more general expressions must be used:[1]

$$D_{F,S}(q) = D_{av}(q) \pm [D_{av}^2(q) - \Delta(D)]^{1/2} \quad (4)$$

where D_F and D_S are the fast and slow diffusion coefficients given by dividing the normal mode decay rates by q^2. D_{av} and $\Delta(D)$ are given by

$$D_{av}(q) = \frac{D_{11}(q) + D_{22}(q)}{2} \quad (5)$$

$$\Delta(D) = D_{11}(q)\, D_{22}(q) - D_{12}(q)\, D_{21}(q) \quad (6)$$

and the terms of the diffusion matrix are given by

$$D_{11} = \frac{D_A^0}{P_A(q)}(1 + 2xC_P A_{2,A} M_{w,A} P_A(q)) \quad (7)$$

$$D_{22} = \frac{D_B^0}{P_B(q)}(1 + 2(1-x)C_P A_{2,B} M_{w,B} P_B(q)) \quad (8)$$

$$D_{12} = 2D_A^0 x C_P A_{2,AB} M_{w,A} \frac{m_B}{m_A} \quad (9)$$

$$D_{21} = 2D_B^0 (1-x) C_P A_{2,AB} M_{w,B} \frac{m_A}{m_B} \quad (10)$$

where D_A^0 (D_B^0) is the single molecule diffusion coefficient of A (B) in a polymer matrix at total polymer concentration C_P, $P_A(q)$ and $P_B(q)$ are the form factors for each component, x is the fraction of the total polymer concentration that is component A, $M_{w,A}$ and $M_{w,B}$ are the molecular weights of the polymers, m_A and m_B are the molecular weights of the monomer units, and $A_{2,A}$ and $A_{2,B}$ are the second thermodynamic virial coefficients for each component in the solvent. $A_{2,AB}$ is the polymer/polymer/solvent second thermodynamic virial coefficient, which gives a measure of the polymer−polymer interactions.

The thermodynamic second virial coefficients for rigid rods like PBLG are not dependent on molecular weight. The value measured by Tracy and Pecora,[8] $(3.9 \pm 0.1) \times 10^{-4}$ cm^3 mol/g^2 for a similar size rod to the one used here, agrees with the average value determined by DeLong and Russo[41] over a series of molecular weights. The solvent in both cases is dimethylformamide (DMF), which is a good solvent. It is assumed that the good solvent chloroform saturated with formamide gives approximately the same virial coefficient. The virial coefficients for flexible polymers like polystyrene are dependent on the molecular weight. Schulz and Lechner[8] measured the virial coefficient for polystyrene (10^5 g/mol) in chloroform. Brown and Nicolai[13] give an expression for the thermodynamic second virial coefficient of polystyrene as a function of the molecular weight in a good solvent. Using a factor of $C^{-0.2}$ to scale the 10^5 g/mol data gives 3.44×10^{-4} cm^3 mol/g^2, nearly the same result as using the Brown and Nicolai equation (3.18×10^{-4} cm^3 mol/g^2) for the 9.51×10^5 g/mol polystyrene used in this study. The average value, $A_2 = 3.31 \times 10^{-4}$ cm^3 mol/g^2, is used below.

B. PBLG/PS/CF. The total polymer concentration was kept at 16.12 mg/mL, and the ratio of the polymer components was varied. We define x as the fraction of the total polymer component that is rods: $x = C_{rod}/C_P$. CONTIN analysis of the DLS data for the PBLG/PS/CF ternary systems shows two modes in all solutions studied. The two decays are identified as diffusive modes because of the linear dependencies of their decay rates on q^2 as shown in Figure 3a,b. Thus, the diffusion coefficients are independent of the scattering vector. The amplitudes of each of these modes also prove to be independent of q. This behavior is the opposite of that observed for the slow mode in the binary solutions of polystyrene in chloroform/formamide, in which both the amplitude and diffusion coefficient are q-dependent.

The diffusion coefficients of the fast mode for the ternary systems containing PBLG are shown in Figure 4a as a function of the rod fraction (x). At $x = 0$ and $q = 0$, the fast diffusion coefficient is the mutual diffusion coefficient of the polystyrene, since this is a binary solution. Similarly, at $x = 1$ and $q = 0$, the binary rod/solvent solution gives the PBLG mutual diffusion coefficient. Between these limits, the diffusion coefficient for collective polymer diffusion is identified as the cooperative diffusion coefficient D_c. The mutual diffusion coefficients for PBLG and polystyrene in chloroform/formamide at 16 mg/mL are $(4.75 \pm 0.01) \times 10^{-11}$ and $(5.50 \pm 0.04) \times 10^{-11}$ m^2/s, respectively. From eqs 4−10, the mutual diffusion coefficients for the binary solutions at $q = 0$ should give $D_F = D_A^0(1 + 2C_P A_{2,A} M_{w,A})$, which would allow calculation of the D_A^0 and D_B^0. For PBLG and polystyrene, $D_A^0 = 2.08 \times 10^{-11}$ m^2/s and $D_B^0 = 4.93 \times 10^{-11}$ m^2/s, respectively. The solid line in Figure 4a is the fit to the data using eqs 4−10 for the fast mode. The mutual diffusion coefficients in the binary solutions are used to determine D_A^0 and D_B^0 so that the only fit parameter is $A_{2,AB} = (4.04 \pm 0.10) \times 10^{-4}$ cm^3 mol/g^2. The Flory χ interaction parameter can be calculated from $A_{2,AB}$.[42] We find $\chi = 0.0073 \pm 0.0022$ (where the error is calculated from the standard deviation to the fit to $A_{2,AB}$).

The diffusion coefficients determined from the slow mode of the ternary systems containing PBLG are shown in Figure 4b as a function of the rod fraction. The slow mode for the binary polystyrene solution is not shown here. In the limit of very low concentration of one of the polymer components, the probe diffusion is measured. Many experiments have been done in which the background polymer matrix is isorefractive with the solvent. The probe diffusion should be the only mode when the background is refractive index matched. In the current experiments, the probe diffusion coefficient should be extrapolated to zero probe concentration. This gives the self-diffusion of one polymer in a

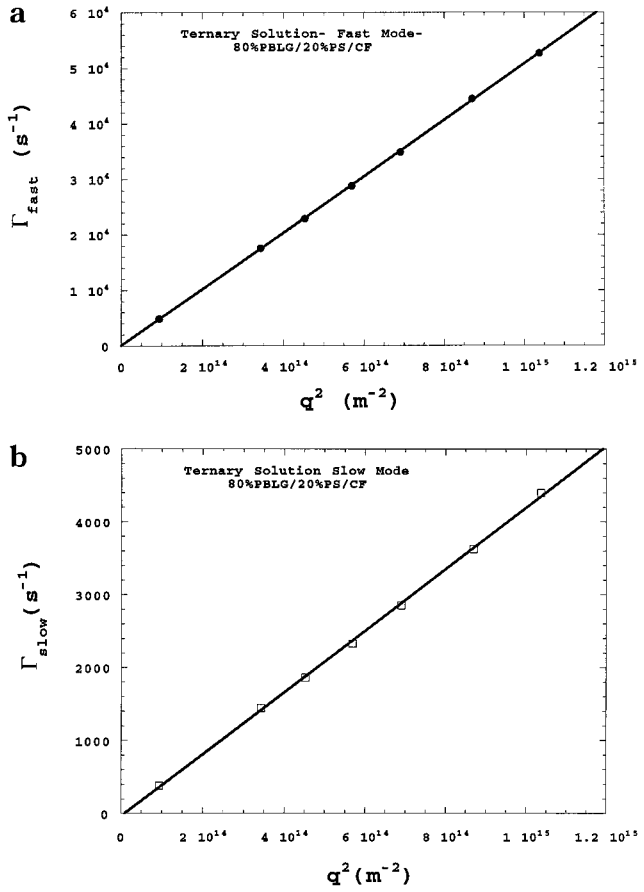

Figure 3. (a) The frequency of the fast mode from the ternary solution 80% PBLG/20% PS vs the square of the scattering vector length. The diffusion coefficient is given as the slope of the linear fit indicated. (b) The frequency of the slow mode from the ternary solution 80% PBLG/20% PS vs the square of the scattering vector length. The diffusion coefficient is given as the slope of the linear fit indicated.

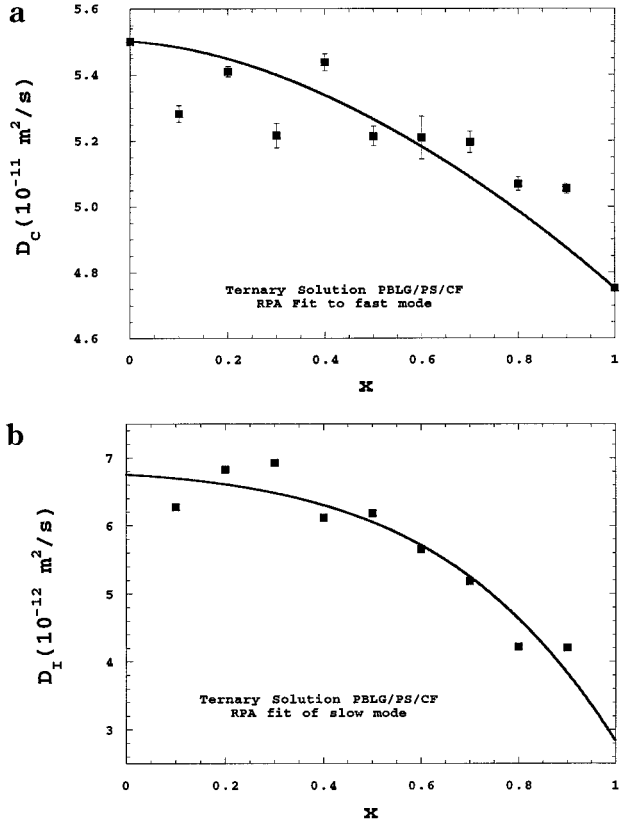

Figure 4. (a) The fast mode diffusion coefficients for the PBLG/PS/CF ternary solutions vs the fraction of PBLG. The line is a fit the RPA equations, using D_A^0 and D_B^0 determined from the binary solutions. (b) The slow mode diffusion coefficients for the PBLG/PS/CF ternary solutions vs the fraction of PBLG. The fit made using the random phase approximation.

background matrix of the other polymer. More generally, the slow mode for ternary solutions will give the interdiffusion coefficient, which represents the relative diffusion of one type of polymer with respect to the other. Equations 4−10 were used to fit the cooperative and interdiffusion coefficients in Figure 4a,b. In addition to the probe self-diffusion coefficients D_A^0 and D_B^0, found close to the values given above, the polymer/polymer/solvent thermodynamic second virial coefficient is determined: $A_{2,AB} = (3.42 \pm 0.30) \times 10^{-4}$ cm^3 mol/g^2, which gives $c = -0.0101 \pm 0.0068$ (where, again, the error is calculated from the standard deviation to the fit that gives $A_{2,AB}$). A negative χ parameter is possible[43−45] and would indicate attraction between the two types of polymer. This suggests that the system is compatible.

The ratio of the amplitudes of the two modes is shown in Figure 5. In the current study, the amplitude ratio is defined as the ratio of the interdiffusion amplitude (slow mode) to the cooperative diffusion amplitude (fast mode). The slow mode amplitude for the 100% polystyrene ($x = 0$) data is not included; the slow mode in the binary PS/CF system is discussed in detail above. The solid line in Figure 5 is the fit to the amplitude data using this general expression for the RPA given by Borsali.[1] The only fit parameter is χ. The fit gives $\chi = -0.023 \pm 0.009$ (where the error given is from the standard deviation to the fit).

According to the DSO theory[4,5] and the modified DSO theory,[46] the D_A^0 value for rigid rods should be the self-

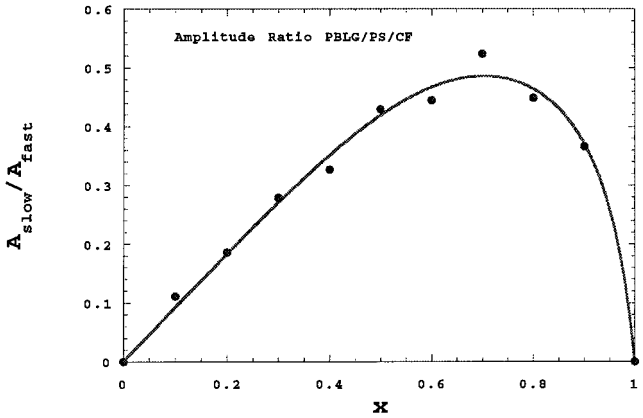

Figure 5. The relaxation mode amplitude ratio for the PBLG/PS/CF ternary system vs the rod fraction. The solid line is the fit to the general expression for the RPA amplitudes (eq 16).

diffusion coefficient. The self-diffusion coefficient of PBLG has been directly measured by Bu et al. using fluorescence bleaching recovery.[47] It was shown that the self-diffusion coefficients are constant up to a concentration C^*, at which the self-diffusion coefficient decreases rapidly with increasing concentration. We can compare the fit results for D_A^0 to the Bu et al. data for $M_w = 103$ kg/mol. The C^* value is 17 mg/mL for this molecular weight, so we can compare their D_{self} at 14.3 mg/mL to our 16.1 mg/mL fits. Accounting for the difference in viscosity, we should expect $D_A^0 = 4.06 \times 10^{-11}$ m^2/s. This is nearly double the value obtained from the RPA fits, but their result is the same as the mutual diffusion

coefficient they measure in less concentrated samples (2−5 mg/mL). Phalakornkul et al.[46] also determined self-diffusion coefficients for PBLG from the mutual diffusion coefficients in a mixed pyridine/dimethylformamide (DMF) solvent. For rod number concentration times L^3 approximately equal to 30 and rod length equal to 68 nm, they found that the self-diffusion coefficient (scaled according to the viscosity of our samples) is $D_A^0 = 2.0 \times 10^{-11}$ m^2/s, in remarkable agreement with the current value ($D_A^0 = 2.08 \times 10^{-11}$ m^2/s, see above). Phalakornkul et al.[46] suggest that the discrepancy in the measured self-diffusion coefficients and those determined from the mutual diffusion coefficients arises because DSO theory does not distinguish between the mutual friction and single rod friction. Bu et al.[47] show that these two frictions are different for PBLG.

As mentioned in the Introduction, the DSO theory is an RPA theory for rigid-rod-like polymers.[4,5] One of the major differences between the rod and coil RPA is that for rods there is the nematic interaction, which is related to the rod−rod side to side contact. This nematic interaction eventually causes solutions of rodlike polymers to become anisotropic. The DSO theory must be considered for both the static and the dynamic contributions in this work. In terms of the static contribution, the nematic interaction does not appear until the q^4 term in the static structure factor (see eq 12). Also, from the SANS data in this study, we expect that all of the static structure factors will be very close to unity in the scattering vector range probed by dynamic light scattering. There is also expected to be no contribution to the relaxation frequency from the nematic interaction term in the low q limit. The extended DSO theory for the main relaxation mode[46] shows that if the relaxation frequency does not deviate from q^2 dependence, then the result is the same as the low q limit of normal DSO.

C. PS/HairyRod/CF. The ternary PBLG/PS/CF solutions were studied at a constant total polymer concentration, and only the relative composition of the two polymer components was varied. In the PS/hairy rod/CF solutions, the polystyrene was always 95% of the total polymer concentration (and the hairy rod 5%). The total polymer concentration was varied from the dilute to the semidilute concentration regime. Two different hairy rods were used. The main difference between them is the fraction of the long alkyl side chains that are referred to as the hairs. The effect of the fraction of side chains on the probe diffusion of the hairy rod in the polystyrene matrix was investigated.

From the CONTIN analysis, we find that there are either one or two peaks. The diffusion coefficient given by the major peak increases with the concentration. The minor peak diffusion coefficient has large errors in the dilute solution, does not appear in the intermediate concentrations near C^*, and then decreases at the highest concentrations studied (see Figure 6a,b). It is thought that the minor peak disappears in the intermediate range because of its small amplitude and because its frequency is close to the one associated with the major peak. The cooperative diffusion process in these ternary solutions, which are 95% PS in composition, is comparable to the cooperative diffusion coefficient measured in the binary PS/CF solutions; this comparison is shown in Figure 7.

In Figure 8a,b, the diffusion coefficients of the two modes from the ternary solutions are compared to the hairy rod binary solution mutual diffusion coefficients.

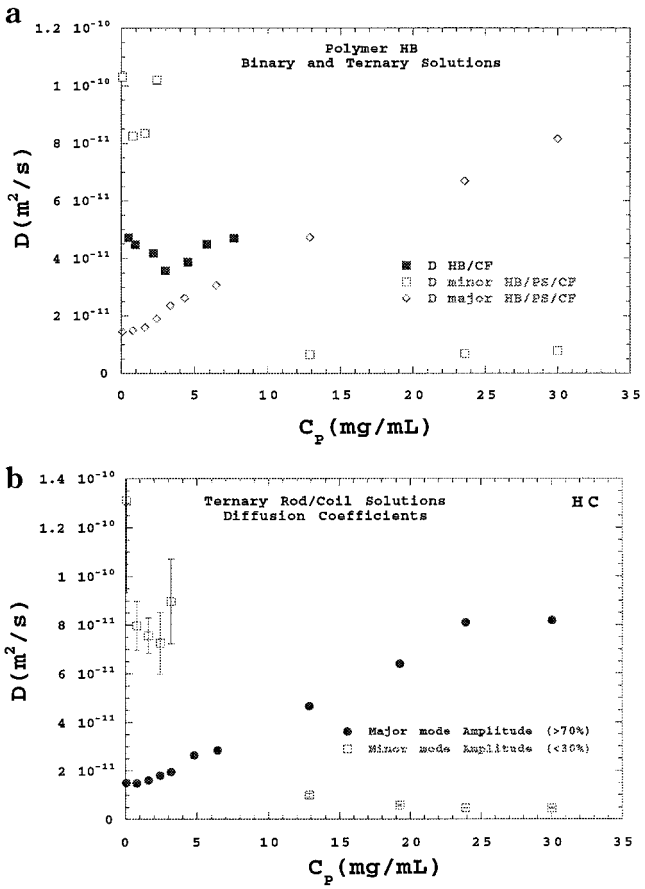

Figure 6. (a) The major (circles) and minor (squares) modes in the ternary solutions HB/PS/CF as determined from the inverse Laplace transform. (b) The major (circles) and minor (squares) modes in the ternary solutions HC/PS/CF as determined from the inverse Laplace transform.

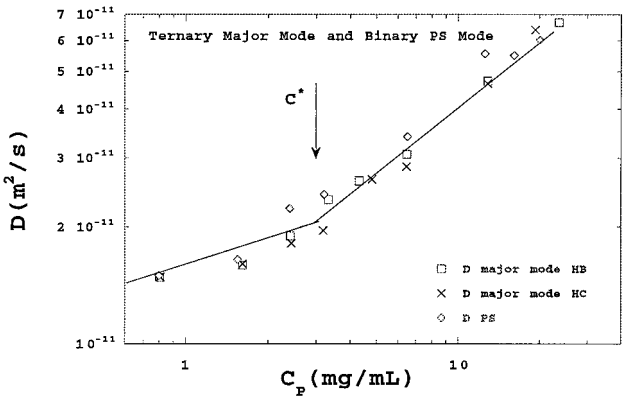

Figure 7. Comparison of the major mode from the binary PS/CF solutions (diamonds) to the major mode determined from the ternary solutions: HB/PS/CF (hollow squares), HC/PS/CF (x symbols).

Figure 9 shows the variation of the interdiffusive mode vs the total polymer concentration for the ternary systems studied: 0% (PBLG), 30% (HC), and 60%(HB) hairy rods in the presence of PS. The probe diffusion coefficient is sensitive to the percentage of hairs on the rod and shows better compatibility as the hair percentage increases. This increase in compatibility follows from the fact that $D_I(60\%) > D_I(30\%)$ and the RPA equations. This result is qualitatively in good agreement, within the error bars, with the negative χ parameters found that would speed up the dynamics.

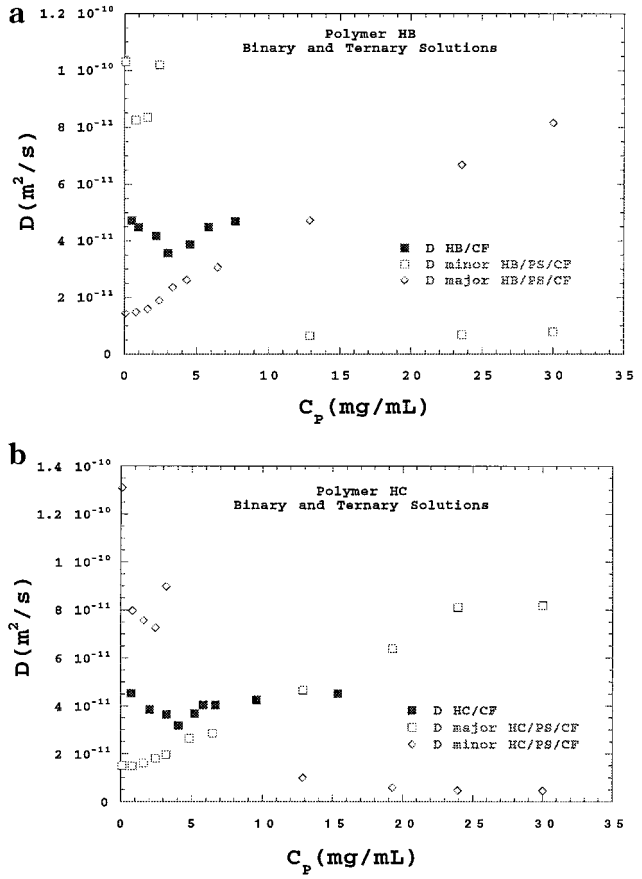

Figure 8. (a) The translational diffusion coefficient of polymer HB in binary solutions (solid squares) compared to the major (diamonds) and minor (hollow squares) modes from the ternary solution HB/PS/CF. (b) The translational diffusion coefficient of polymer HC in binary solutions (solid squares) compared to the major (hollow squares) and minor (diamonds) modes from the ternary solution HC/PS/CF.

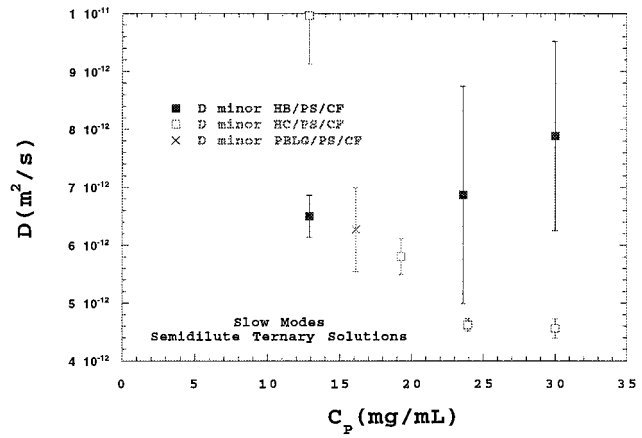

Figure 9. The interdiffusive ("fast mode") vs the total polymer concentration for ternary rod solutions containing 0% (PBLG), 30% (HC), and 60% (HB) octadecyl hairs.

V. SANS Results

Small-angle neutron scattering (SANS) experiments were used to investigate the structure of the polymer solutions and particularly to determine the Flory interaction parameter χ. All solutions with total polymer concentration 32.2 mg/mL are in the semidilute concentration regime. The important length scale in semidilute solutions is the correlation length ξ. In the semidilute regime, solution properties should be dependent upon the total polymer concentration. Results for ternary solutions are compared to results for the binary solutions using the random phase approximation (RPA). Temperature effects are considered for the PBLG binary solutions as well as for the 50%/50% ternary solutions. The concentration dependence was considered for both the binary PBLG and the binary polystyrene solutions. Two experimental configurations were used in order to extend the scattering vector range probed.

Table 2. SANS Results on PBLG and PS Binary Solutions

sample	conc (mg/mL)	T (°C)	ξ (Å)	K (10^4 Å^4)
PBLG	32.2	28	21.68 ± 0.43	1.37 ± 0.20
PBLG	32.2	20	23.18 ± 0.66	2.65 ± 0.46
PBLG	32.2	12	23.85 ± 0.54	5.66 ± 0.88
PBLG	32.2	0	22.64 ± 0.46	2.54 ± 0.58
PBLG	32.2	−12	22.57 ± 0.50	2.11 ± 0.39
PBLG	32.2	15	24.9 ± 1.7	
PBLG	7	20	65 ± 8	
PBLG	3.7	20	89 ± 10	
PS	32.2	20	26.3 ± 1.0	
PS	7	20	74.9 ± 2.5	

A. PBLG and PS in Binary Solutions. The correlation length ξ for semidilute solutions of Gaussian coil polymers can be determined from the static structure factor $S(q)$:[32]

$$1/S(q) = [1/S(0)](1 + q^2\xi^2) \tag{11}$$

This expression is the Fourier transform of the pair correlation function, which decays exponentially with distance. The structure factor is proportional to the intensity of the scattering $I(q)$. Shimada, Doi, and Okano have given a corresponding expression applicable to semidilute rigid rods:[5]

$$1/S(q) = [1/S(0)](1 + \xi^2q^2 + Kq^4 + ...) \tag{12}$$

SANS data obtained on the PS and the PBLG were analyzed according to these equations. The results are shown in Table 2. We do not discuss the PS results since they are in good agreement with studies in the literature. We discuss the PBLG data in more detail. In the lower q region, the variation of $1/I(q)$ vs q^2 was clearly linear, and so the q^4 term was not used in these fits. For the high q region, K is determined using the ξ from the fit to the lower q region.

K is a measure of the nonlinearity in a plot of $1/S(q)$ vs q^2. DSO[4,5] have given its dependence on the rod number density ν:

$$K = L^4\frac{7 - 27\left(\frac{\nu}{\nu^*}\right)}{32400\left(1 - \left(\frac{\nu}{\nu^*}\right)\right)} \tag{13}$$

where ν^* is the number concentration at which the isotropic phase becomes unstable. An important property of K is that it changes sign from positive to negative as the rod concentration is increased. The inversion takes place at $(7/27)C_c$, where C_c is the critical mass concentration at which the isotropic phase becomes unstable.

The values of the correlation length can be compared with the results of DeLong and Russo for PBLG in DMF.[41] They give a relationship between rod length, correlation length, and number concentration:

$$(L/6\xi)^2 = 1 + 8\nu/\nu^* \tag{14}$$

This equation fits their data up to approximately $\nu/\nu^* = 0.2$. Above this concentration, the correlation length becomes difficult to reliably measure with visible light. Our PBLG solutions have $\nu/\nu^* = 0.23$, and from a rod length of 700 Å, we would expect a correlation length of 69 Å. Our measured ξ are much lower than this value, and this large discrepancy is unexplained at this point. It should be noted that, above $\nu/\nu^* = 0.2$ in the DeLong and Russo work (Figure 2), data points vary wildly from this expression. Our SANS determined correlation lengths agree with the data of Tracy and Pecora.[8] For a 20.9 mg/mL PBLG solution in DMF, static light scattering measurements give $\xi = 34.0$ Å ($M_w \sim 5\%$ higher than in this study). Assuming that $\xi \propto C^{0-.5}$ and $\xi \propto L$, this would correspond to $\xi = 26$ Å for our system.

The dilute PBLG solution experiments were studied only in the second SANS configuration described in the Experimental Section. The data were fit to the reciprocal of the first equation since the poor statistics on top of an already weak signal leads to large-magnitude fluctuations (both positive and negative) when $1/I(q)$ is considered. The ξ values are greater than for the highest concentration but have not yet reached the value expected for the dilute solutions. The concentration for each of these solutions is still well above the overlap concentration, C^*. In the dilute limit, the ξ_{app} determined from the equations above should be equal to $L/6$, giving $\xi_{app} = 103$ Å. The less concentrated solutions are more consistent with the equation given by DeLong and Russo above. They also show good agreement with the series of concentrations studied by Tracy and Pecora.

B. Ternary PBLG/PS/CF. The static version of the RPA was used to analyze the SANS data for the ternary solutions. The following discussion is based on the review of the RPA by Borsali,[1] with the specific example of two homopolymers in a solvent. The total structure factor $S_T(q)$ is given by

$$S_T(q) = \sum_{i,j=1}^{2} a_i a_j S_{ij}(q) \tag{15}$$

where the $S_{ij}(q)$ are the components of the static structure factor matrix and a_i is the contrast between polymer i and the solvent. For light scattering, the contrast is the refractive index increment, and for neutron scattering, it is the difference in the scattering length density. The components of the static structure factor matrix are given by

$$S_{11}(q) = \frac{S^0_{11}(q)[1 + \nu_{22} S^0_{22}(q)]}{D} \tag{16}$$

$$S_{12}(q) = S_{21}(q) = \frac{-\nu_{12} S^0_{11}(q)\, S^0_{22}(q)}{D} \tag{17}$$

where $S_{22}(q)$ is obtained by exchanging the indices of $S_{11}(q)$, and the denominator is given by

$$D = 1 + \nu_{11} S^0_{11}(q) + \nu_{22} S^0_{22}(q) + (\nu_{11}\nu_{22} - \nu^2_{12}) S^0_{11}(q)\, S^0_{22}(q) \tag{18}$$

The ν_{ii} are the excluded-volume parameters between the solvent and the polymer. The polymer−polymer excluded-volume parameter is given as ν_{12}. The bare structure factors are given by

$$S^0_{11}(q) = x\Phi_P N_1 P_1(q) \tag{19}$$

and

$$S^0_{22}(q) = (1 - x)\Phi_P N_2 P_2(q) \tag{20}$$

where Φ_P is the total polymer volume fraction, x the part of the polymer fraction that is component 1 (PBLG), N_i the number of monomers per polymer, and $P_i(q)$ the intramolecular form factors for homopolymer i. The $P_{coil}(q)$ for the coils were assumed to follow the Debye function for Gaussian chains:

$$P_{coil}(q) = \frac{2}{u_i^2}(\exp(-u_i) + u_i - 1) \tag{21}$$

where $u_i = (qR_g)^2$ and R_g is the radius of gyration of the coil. The form factor for the rods is

$$P_{rod}(q) = \frac{2}{qL}\int_0^{qL/2} \frac{\sin x}{x}\, dx - \left(\frac{\sin\left(\frac{qL}{2}\right)}{\frac{qL}{2}}\right)^2 \tag{22}$$

Calculation of the volume fraction and degree of polymerization (N_i) is trivial. The calculation of the excluded volume is more difficult. The terms with the excluded volume can be simplified using

$$\nu_{ii}\Phi_P N_i = 2A_{2,i} M_i C_P \tag{23}$$

where $A_{2,i}$ is the second thermodynamic virial coefficient of component i and M_i the molecular weight of i. From eq 23, we find $\nu_{PBLG} = 0.2161$ and $\nu_{PS} = 0.073\,78$. From the experimental SANS data and the above equations, the polymer−polymer excluded-volume parameter can be determined. This can then be compared to the results for the second thermodynamic virial coefficient, $A_{2,12}$, determined by DLS.

First the binary SANS data was fit using the above equations and $x = 1$ for PBLG/CF (Figure 10a) and $x = 0$ for PS/CF (Figure 10b). From these fits, the $R_{g,i}$ and ν_{ii} were determined. Using only ν_{12} as a fit parameter, the ternary solution data was fit for the 50% PBLG/50% PS/CF (Figure 11a) and the 60% PBLG/40% PS/CF (Figure 11b), giving almost identical values for the polymer−polymer excluded-volume parameter: $\nu_{12} = 0.127 \pm 0.006$ and 0.125 ± 0.006, respectively. This polymer−polymer excluded-volume parameter is the same as the geometric mean of the individual polymer−solvent excluded volumes $(\nu_{PBLG}\nu_{PS})^{0.5} = 0.126$. This gives the polymer−polymer virial coefficient $A_{2,12} = (3.59 \pm 0.17) \times 10^{-4}$, which is very close to the value determined from the analysis of the dynamic light scattering data; the Flory interaction parameter from this $A_{2,12}$ value is $\chi = -0.0025 \pm 0.0039$.

VI. Conclusions

Binary solutions of polystyrene in chloroform saturated with formamide were studied in the dilute to semidilute regime. The major relaxation mode followed the expected behavior for the translational diffusion of the random coil polymer. A weak slow mode was observed in solutions that are highest in concentration

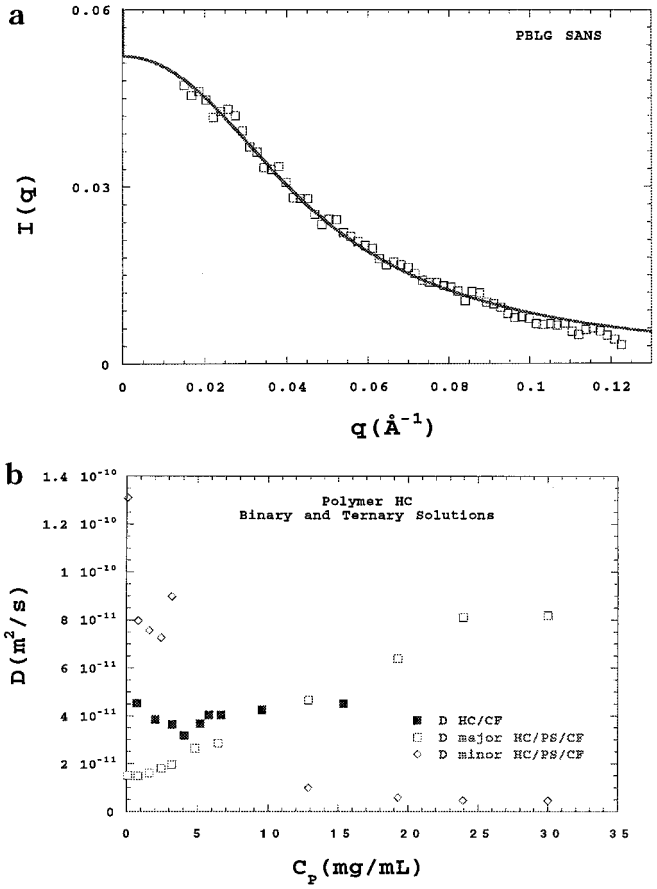

Figure 10. (a) The small-angle neutron scattering for PBLG. The solid line is a fit to the RPA equations in the limit that the fraction of PBLG = 1. (b) The small-angle neutron scattering from polystyrene, fit to the RPA equations in the limit that the fraction of PBLG = 0.

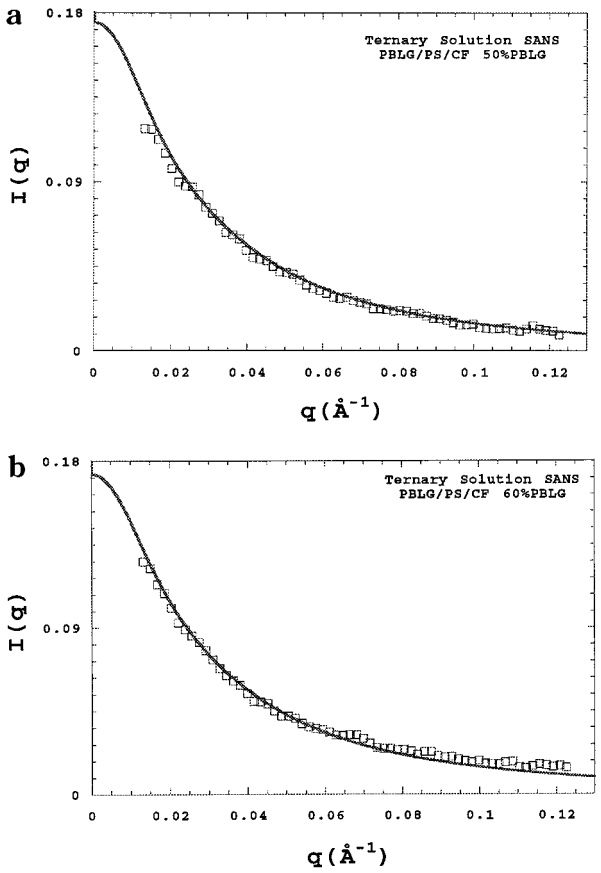

Figure 11. (a) The small-angle neutron scattering of ternary solution 50% PBLG/50% PS/CF. The solid line is a fit using the RPA equations. (b) The small-angle neutron scattering of ternary solution 60% PBLG/40% PS/CF. The solid line is a fit using the RPA equations.

and at the highest scattering angles. The frequency of this slow relaxation appears to be proportional to q^3, as opposed to the expected q^2 dependence for translation. Possible causes of this slow mode were discussed. The binary solutions of hairy rodlike polymers in chloroform (with formamide) were studied previously.[7] Our studies of semidilute binary solution of PBLG in chloroform (with formamide) gives comparable results for the mutual diffusion coefficient to those for the hairy rods.

The ternary solutions of PBLG/PS/CF exhibit two diffusive modes in the dynamic light scattering experiments, as expected from the RPA theory. The diffusion coefficients determined and their amplitudes are independent of the scattering vector. The two modes are identified as the cooperative diffusion and the interdiffusion modes. The cooperative mode is related to the relaxation of total polymer concentration fluctuations; the interdiffusion mode is related to the relaxation of composition fluctuations. The cooperative diffusion coefficient becomes the mutual diffusion coefficient in the limits of $x = 0$ and $x = 1$ (at $q = 0$). It is shown that the D_A^0 for PBLG is not the same as the self-diffusion coefficient. The equality is suggested for rigid-rod polymers by the DSO theory, although the mutual frictional coefficient and the single rod frictional coefficient are assumed to be equal in this theory. The probe diffusion coefficients are determined from the extrapolation of the slow mode data. The amplitude ratio is well described by the RPA, which gives a consistent interpretation of the experiments.

SANS was used to investigate the solution structure. The static correlation lengths (ξ) were determined for binary and ternary solutions. The ξ for binary PBLG/CF solutions compared well with the static light scattering data of Tracy and Pecora for PBLG in DMF. The RPA was used to fit the static structure factor for the ternary solutions.

The Flory interaction parameter χ was determined in four different ways for the PBLG/PS/CF ternary solutions using the RPA model. The χ parameter was determined from the cooperative diffusion mode (−0.0101), the interdiffusion mode (0.0073), the amplitude ratio (−0.023), and the small-angle neutron scattering (−0.0025). These values are remarkably close given the simplicity of the theory and the possible errors in the DLS and SANS experiments. The closeness is another example of the consistency of the RPA approach. They suggest that the interaction parameter is very small and likely slightly negative. A negative interaction parameter indicates attraction between polymer components in the given solvent, which favors polymer−polymer miscibility.[48,49]

The probe diffusion coefficient (from the interdiffusive mode) of the hairy rods was measured in the ternary hairy rod/PS/solvent systems as a function of the total polymer concentration in the semidilute regime. Near the overlap concentration, the probe diffusion peak was not observed. This is likely due to the closeness of this weak peak to the cooperative diffusion peak. In the dilute solutions, the major mode is still comparable to the polystyrene diffusion mode. The interdiffusive mode

relaxes faster as the percentage of hairs on the rod is increased. This is an indication that the hairs increase the compatibility of the rods with the PS in this solvent.

Acknowledgment. We thank Dr. Boualem Hammouda of NIST for his help with the SANS experiments and Dr. Hilde von Esbroeck and Professor Curtis Frank of Stanford University for providing us with the hairy rod polymers**.** This work was partially supported by NATO Cooperative Linkage Grant 975728 and National Science Foundation (USA) Grant CHE-9520845.

References and Notes

(1) Borsali, R. *Macromol. Chem. Phys.* **1996**, *197*, 3947.
(2) Cantor, A. S.; Pecora, R. *Macromolecules* **1994**, *27*, 6817.
(3) Jamil, T.; Russo, P. S.; Negulescu, I.; Daly, W. H.; Schaefer, D. W.; Beaucage, G. *Macromolecules* **1994**, *27*, 171.
(4) Doi, M.; Shimada, T.; Okano, K. *J. Chem. Phys.* **1988**, *88*, 4070.
(5) Shimada, T.; Doi, M.; Okano, K. *J. Chem. Phys.* **1988**, *88*, 2815.
(6) Doty, P. J.; Bradbury, J. H.; Holtzer, A. M. *J. Am. Chem. Soc.* **1956**, *18*, 947.
(7) Hanson, E. T.; Pecora, R. *J. Phys. Chem. B*, submitted.
(8) Tracy, M. A.; Pecora, R. *Macromolecules* **1992**, *25*, 337.
(9) Provencher, S. W. *Comput. Phys. Commun.* **1982**, *27*, 213, 229.
(10) Schulz, G. v.; Lechner, M. In *Light Scattering From Polymer Solutions*; Huglin, M. B., Ed.; Academic Press: New York, 1972.
(11) Brown, W. *Polymer* **1984**, *25*, 680.
(12) Borsali, R.; Duval, M.; Benoit, H.; Benmouna, M. *Macromolecules* **1987**, *20*, 1112.
(13) de Gennes, P. G. M*acromolecules* **1976**, *9*, 594.
(14) Stockmayer, W. H.; Hammouda, B. *Pure Appl. Chem.* **1984**, *56*, 1373.
(15) Brown, W.; Nicolai, T. *Colloid Polym. Sci.* **1990**, *268*, 977.
(16) Amis, E. J.; Han, C. C. *Polymer* **1982**, *23*, 1403.
(17) Brown, W.; Johnsen, R. M. *Macromolecules* **1985**, *18*, 379.
(18) Chu, B.; Nose, T. *Macromolecules* **1980**, *13*, 122.
(19) Callaghan, P. T.; Pinder, D. N. *Macromolecules* **1980**, *13*, 1085.
(20) Fleischer, G.; Zgadzai, O. E.; Skirda, V. D.; Maklakov, A. I. *Colloid Polym. Sci.* **1988**, *266*, 201.
(21) Hervet, H.; Legér, L.; Rondelez, F. *Phys. Rev. Lett.* **1979**, *42*, 1681.
(22) Nemoto, N.; Makita, Y.; Tsunashima, Y.; Kurata, M. *Macromolecules* **1984**, *17*, 2629.
(23) Brown, W.; Johnsen, R. M.; Stilbs, P. *Polym. Bull.* **1983**, *9*, 305.
(24) Brown, W. *Macromolecules* **1984**, *17*, 66.
(25) Brown, W.; Stepánek, P. *Macromolecules* **1988**, *21*, 1791.
(26) Burchard, W.; Eisele, M. *Pure Appl. Chem.* **1984**, *56*, 1379.
(27) Wenzel, M.; Burchard, W.; Schätzel, K. *Polymer* **1986**, *27*, 195.
(28) Delsanti, M.; Chang, J.; Lesieur, P.; Cabane, B. *J. Chem. Phys.* **1996**, 7200.
(29) Wang, C. H. *Macromolecules* **1992**, *25*, 1524.
(30) Wang, C. H. *J. Chem. Phys.* **1995**, *102*, 6537.
(31) Wang, C. H.; Sun, Z.; Huang, Q. R. *J. Chem. Phys.* **1996**, *105*, 6052.
(32) Brown, W.; Stepánek, P. *Macromolecules* **1993**, *26*, 6884.
(33) Adam, M.; Delsanti, M. *Macromolecules* **1977**, *10*, 1229.
(34) Adam, M.; Delsanti, M. *Macromolecules* **1985**, *18*, 1760.
(35) Chu, B.; Nose, T. *Macromolecules* **1980**, *13*, 122.
(36) Doi, M.; Edwards, S. F. *The Theory of Polymer Dynamics*; Clarendon Press: Oxford, 1986; Chapter 4, pp 91−139.
(37) de Gennes, P. G. *Scaling Concepts in Polymer Physics*; Cornell University Press: Ithaca, NY, 1979; Chapter 6, pp 165−204.
(38) Akcasu, A. Z.; Gurol, H. *J. Polym. Sci.* **1976**, *14*, 1.
(39) Akcasu, A. Z.; Benmouna, M.; Han, C. C. *Polymer* **1980**, *21*, 866.
(40) Lodge, T. P.; Han, C. C.; Akcasu, A. Z. *Macromolecules* **1983**, *16*, 1180.
(41) DeLong, L. M.; Russo, P. S. *Macromolecules* **1991**, *24*, 6139.
(42) Sun, Z.; Wang, C. H. *J. Chem. Phys.* **1997**, *106*, 3775.
(43) Avella, M.; Martuscelli, E. *Polymer* **1988**, *29*, 1731.
(44) Kawahara, S.; Sato, K.; Akiyama, S. *J. Polym. Sci., Part B: Polym. Phys.* **1994**, *32*, 15.
(45) Robledo-Muniz, J. G.; Tseng, H. S.; Lloyd, D. R. *Polym. Eng. Sci.* **1985**, *25*, 934.
(46) Phalakornkul, K. J.; Gast, A. P.; Pecora., R. *Macromolecules* **1999**, *32*, 3122.
(47) Bu, Z.; Russo, P. S.; Tipton, D. L.; Negulescu, I. I. *Macromolecules* **1994**, *27*, 6871.
(48) Olabisi, O.; Robeson, L. M.; Shaw, M. T. *Polymer−Polymer Miscibility*; Academic Press: San Francisco, 1979.
(49) Ould-Kaddour, L.; Strazielle, C. *Eur. Polym. J.* **1988**, *24*, 117.

MA001857J